

LETTER TO THE JOURNAL

Single-cell landscape of malignant ascites from patients with metastatic colorectal cancer

The presence of malignant ascites in colorectal cancer (CRC) patients is associated with a poor prognosis, a high risk of recurrence, and resistance to chemotherapy and immune therapy [1–3]. Understanding the complex interactions among different kinds of cells and the ecosystem of peritoneal metastasized colorectal cancer (pmCRC) ascites may provide insights into effective treatment strategies.

We profiled the single-cell transcriptomes of 96,065 cells from ascites samples of 12 treatment-naïve patients with pmCRC using the 10× single-cell RNA-sequencing (scRNA-seq) (Supplementary Figure S1A, Supplementary Table S1). Eleven major cell types were identified by characteristic canonical cell markers, including epithelial cells, endothelial cells, fibroblasts, T cells, B cells, monocytes, macrophages, plasma cells, natural killer (NK) cells, dendritic cells (DCs), and mast cells (Figure 1A–B). The main cellular components of pmCRC ascites are T cells (40,095; 41.7%), macrophages (28,487; 29.7%), and fibroblasts (5,932; 6.2%). Compared with primary CRC, which showed 14.8% epithelial cells [4], only 0.3% (291) epithelial cells were found in the ascites. The low percentage of epithelial cells in pmCRC ascites was consistent with the scRNA-seq studies of another tumor ascites [5–7].

We classified the 12 patients into 2 groups according to their treatment response as follows: 8 patients (P02, P03, P04, P07, P08, P09, P11, and P12) had stable disease (SD), while 4 (P01, P05, P06, and P10) had progressive disease (PD). Single-cell transcriptomic analyses have revealed high heterogeneity of cell composition in 12 patients. The SD group exhibited a higher proportion of fibroblasts and epithelial cells (Figure 1B). Remarkably, fibroblasts had significantly different expression characteristics between the 2 groups (Figure 1C), and the top five upregulated/downregulated genes were visualized in 11 cell types (Figure 1D). We also found a significant increase in the frequency of macrophages in pmCRC ascites compared with the primary tumors [4] (Figure 1E). It hinted that significant inter-patient variability in the

composition and functional programs of pmCRC ascites cells under different disease states.

To comprehensively study the cellular interactions within the pmCRC ascites ecosystem, we predicted cell-cell communication networks using CellChat. Overall, we identified 44 significant ligand-receptor pair interactions. Although T cells were the most abundant cell population (41.7%) in pmCRC ascites, fibroblasts and macrophages were the core of the cellular interaction network (Figure 1F), suggesting their important roles in recruiting and cross-talking with diverse cells in the pmCRC ascites ecosystem.

The result of cellular communications suggested that there was a complex interplay between various signaling molecule. Macrophage migration inhibitory factor (MIF), annexin, complement, and C-C chemokine ligand (CCL) were the most active outgoing/incoming signaling molecules in CRC ascites (Supplementary Figure S1B). Fibroblasts directly contacted with different types of cells via ligand-receptor interactions of the MIF-(CD74 + C-X-C chemokine receptor type 4 [CXCR4]) and MIF-(CD74 + CD44) axes and C3-(integrin alpha X [ITGAX] + integrin subunit beta 2 [ITGB2]) (Figure 1G). Notably, macrophage populations were more likely to interact with other cells through the adhesive ligand-receptor pairs galectin-9 (LGALS9)-CD44 and LGALS9-CD45, which were not observed in other cell populations (Figure 1G). CD74, LGALS9 were significantly associated with metastasis in The Cancer Genome Atlas (TCGA) CRC cohorts. We also found CD44 and ITGAX were survival (Figure 1H; CD44 and ITGAX showed no significant differential expression between metastatic and non-metastatic patients, so data are not shown). These results indicated that the entire cellular interaction network of pmCRC ascites contributed to establishing an immunosuppressive and metastatic microenvironment.

We observed that the abundance of fibroblasts in pmCRC ascites samples was significantly greater in SD

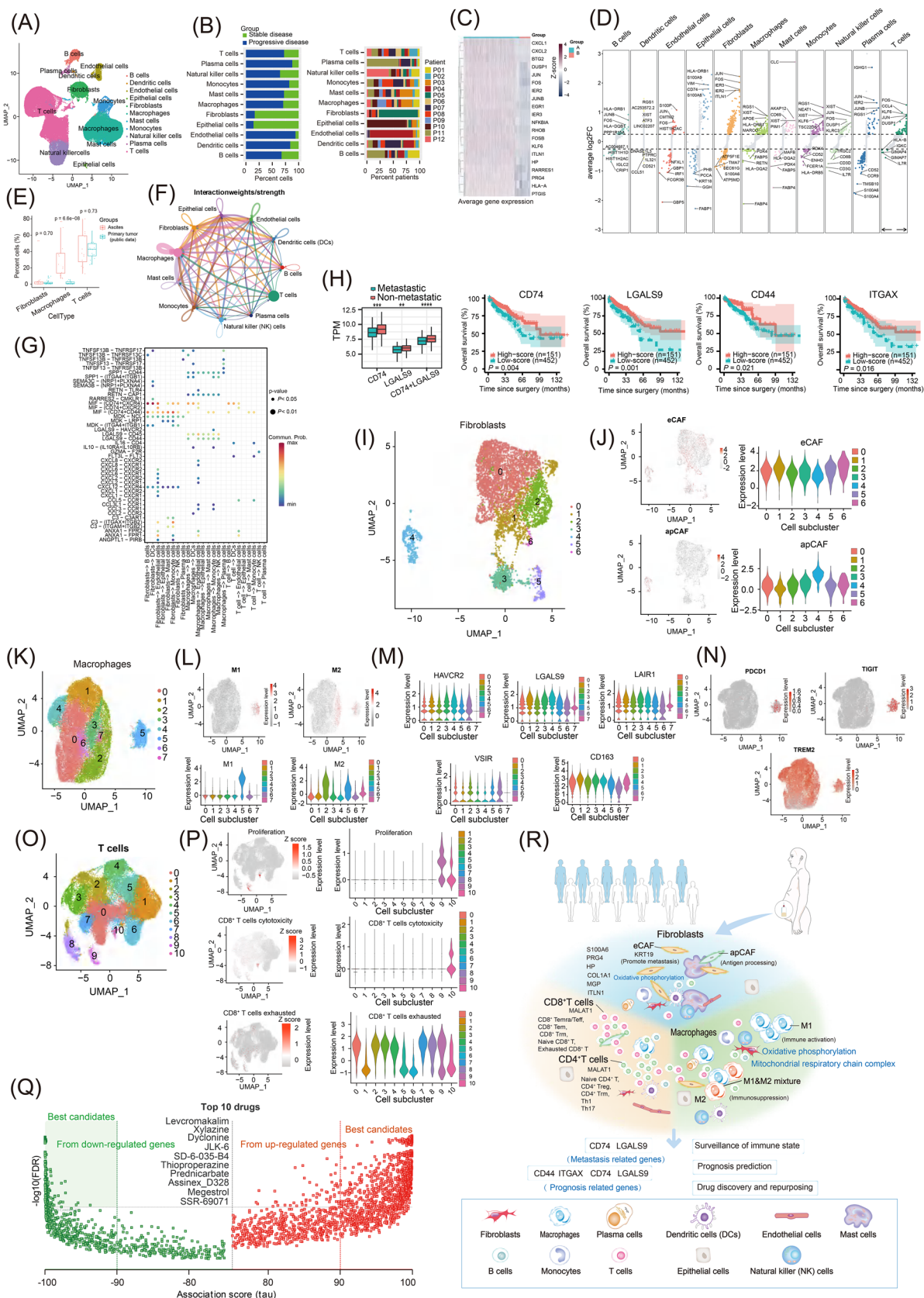


FIGURE 1 Single-cell transcriptomic landscape of malignant ascites of metastatic CRC. (A) The UMAP plot shows 11 major cell types in pmCRC ascites, color-coded by cell types. (B) The fraction of each major cell type across 12 patients between PD and SD patients shows heterogeneous (left panel). The fraction of each patient across 11 cell type populations shows heterogeneous (right panel). (C) Differential gene expression of fibroblasts between PD and SD patients. (D) Differential gene expression reveals significantly up-regulated and

patients than in PD patients (Figure 1B). The fibroblasts were partitioned into 7 distinct clusters (C0-C6) based on unsupervised clustering (Figure 1I). All sub-clusters of cancer-associated fibroblasts (CAFs) showed a high expression of extracellular matrix cancer-associated fibroblasts (eCAFs) signature (Figure 1J), while inflammatory CAF (iCAF), myofibroblast CAF (myCAF), matrix CAF (mCAF), and vascular CAF (vCAF) only presented in a small fraction of fibroblasts (Supplementary Figure S1C), supporting the role of eCAFs in enhancing the metastatic potential of pmCRC. A higher abundance of antigen-presenting cancer-associated fibroblasts (apCAFs) was observed in the PD cohort ($n = 310$) than in the SD cohort ($n = 93$) (Wilcoxon test, $P = 0.049$). These results indicated that the CAFs in pmCRC ascites have bidirectional associations with immune regulation function, serving as a favorable candidate for CRC treatment. Differentially expressed genes and gene ontology (GO) analyses showed that the “cell-cell adhesion”, “inflammatory response”, and “cytokine production” were differentially enriched between primary tumors and ascites (Supplementary Figure S1D), which implied that the liquid state of ascites changed the functions of the fibroblast populations.

Macrophages were significantly enriched in pmCRC ascites and categorized into 8 sub-clusters (C0-C7) (Figure 1K). Using the previously defined “M1” and “M2” signatures, C2 showed an “M1-like” pattern, and C5 showed “M2-like” patterns. We also identified a small sub-cluster of C5 co-expressed both “M1” and “M2” gene signatures (Figure 1L), which have been reported in previous studies on solid tumors [8]. We next

examined the expression of a series of the previously reported immunosuppressive genes (leukocyte-associated immunoglobulin-like receptor 1 [LAIR1], hepatitis A virus cellular receptor 2 [HAVCR2; also known as T cell immunoglobulin and mucin domain-containing protein 3], LGALS9, and V-set immunoregulatory receptor [VSIR]) in macrophage sub-clusters. Because the expression pattern of the “M2” marker gene CD163 perfectly coincided with that of LAIR1 in all sub-clusters (Figure 1M), we postulated that the immunosuppressive function of tumor-associated macrophages (TAMs) might be exerted via LAIR1. Two other immunosuppressive genes, T cell immune receptor with Ig and ITIM domains (TIGIT) and programmed cell death 1 (PDCD1), were also identified highly expressed in C5. C4 highly expressed the key immunosuppressive phenotypic marker triggering receptor expressed on myeloid cells 2 (TREM2) (Figure 1N). In summary, the majority of macrophages in pmCRC ascites exhibited high immunosuppressive features.

We identified 11 sub-clusters of T cells according to the expression of their respective markers, including CD4⁺ T cells (C1, C4, C5, and C6) and CD8⁺ T cells (C0, C2, C3, C7, C8, C9, and C10) (Figure 1O). Most CD8⁺ effector memory cells re-expressing CD45RA T (Temra/Teff) cells (C8) were from patient 5 (P05), and CD8⁺ effector memory T (Tem) cells (C7) were mostly from patient 8 (P08); the remaining 10 patients exhibited high heterogeneity in 11 T-cell sub-clusters (Supplementary Figure S1E-F). Importantly, CD8⁺ tissue-resident memory (Trm) cells (C7), which were reported to be associated with forming a tertiary lymphoid structure (TLS) [9], were less abundant

down-regulated genes in 11 cell types between PD and SD patients. (E) Comparison of cell abundance between primary tumor and ascites. Macrophages are significantly more abundant in ascites than in primary tumors. The data of primary tumor were cited from Khailq *et al.* (2022) Genome Biology (<https://doi.org/10.1186/s13059-022-02677-z>) (F) Circle plots show the cellular interaction network of 11 cell types in pmCRC ascites. Fibroblasts and macrophages were the core of the cellular interaction network (Edge width represents the numbers of interactions and node size represents the abundance of cell populations. The round loops along with cell type represent the interactions within the same cell type.). (G) Dot plots show communication probability of the interactions between cell populations in pmCRC ascites (The dot size is proportional to the contribution score computed from pattern recognition analysis.). (H) The box plots show CD74, LGALS9 and both were highly expressed in metastatic patients of TCGA COAD & READ patients. The Kaplan-Meier overall survival curves of CD74, LGALS9, CD44 and ITGAX using TCGA COAD & READ patients. High score, $n = 151$; low score, $n = 452$. (I) UMAP plot of fibroblasts are grouped into 7 cell sub-clusters and indicated by color. (J) UMAPs show the expression levels of eCAFs scores and apCAFs scores in fibroblasts. Violin plots show the expression levels of eCAFs scores and apCAFs scores in fibroblasts sub-clusters. (K) UMAP plot of macrophages are grouped into 8 cell sub-clusters and indicated by color. (L) UMAPs and violin plots show the M1/M2 score in macrophages sub-clusters. (M) Violin plots show the upregulations of multiple immunosuppressive markers, HAVCR2, LGALS9, LAIR1, VSIR and cancer-promoting M2-like macrophage marker (CD163). (N) UMAPs show the enriched expression for PDCD1, TIGIT and TREM2. (O) UMAP plot of T cells are grouped into 11 cell sub-clusters and indicated by color. (P) UMAPs and violin plots show the enrichment of the proliferation score, CD8⁺ T cells cytotoxicity score and CD8⁺ T cells exhausted score in T cells sub-clusters. (Q) The single cell transcriptomics landscape of pmCRC ascites. (R) Drug repurposing using the transcriptomes data of macrophages in pmCRC ascites, shows 10 best drug candidates. Abbreviations: apCAF, antigen-presenting cancer-associated fibroblast; CRC, colorectal cancer; eCAF, extracellular matrix cancer-associated fibroblast; HAVCR2, hepatitis A virus cellular receptor 2; ITGAX, integrin alpha X; LAIR1, leukocyte-associated immunoglobulin-like receptor 1; LGALS9, recombinant human galectin-9; PD, progressive disease; PDCD1, programmed cell death 1; pmCRC, peritoneal metastasized colorectal cancer; SD, stable disease; TIGIT, T cell immune receptor with Ig and ITIM domains; TREM2, triggering receptor expressed on myeloid cells 2; UMAP, uniform manifold approximation and projection; VSIR, V-set immunoregulatory receptor.

in SD patients (P03, P08, P09, P11, and P12). We also observed that all sub-clusters expressed ferritin light chain (FTL) (Supplementary Figure S1G), which was reported to regulate chemoresistance and metastasis in CRC [10]. We calculated the cytotoxicity, proliferation, and exhaustion signatures for all CD8⁺ T-cell sub-clusters (Figure 1P). Only one sub-cluster of CD8⁺ T cells was not show exhaustion signature (C10). Clusters 9 and 10 exhibited slightly higher proliferation, which could recruit cytotoxic T cells. The abundance of C9 and C10 was low, suggesting that T cells may play a minor role in the immune microenvironment of ascites and may work synergistically with other cell populations. Moreover, we predicted immunomodulatory drugs targeting macrophages, where gene sets were extracted from the macrophages of the pmCRC ascites data (Figure 1Q).

In conclusion, we found that T cells, fibroblasts, and macrophages exhibited immunosuppressive features in pmCRC ascites (Figure 1R). The cellular landscape of pmCRC ascites has the significant indication of patients' immune status, providing insights for prognosis and therapy selection.

AUTHOR CONTRIBUTIONS

Haiyang Zhou made contributions to the conceptualization, funding acquisition, investigation, resource acquisition, and writing original draft.

Jiahui Yin made contributions to the data curation, formal analysis, and software analysis.

Anqi Wang made contributions to the formal analysis, investigation, and resource acquisition.

Xiaomao Yin made contributions to the formal analysis.

Taojun Jin made contributions to the formal analysis and visualization.

Kai Xu made contributions to the resource acquisition and supervision.

Lin Zhu made contributions to the investigation and resource acquisition.

Jiexuan Wang made contributions to the investigation and resources acquisition.

Wenqiang Wang made contributions to the resource acquisition.

Wei Zhang made contributions to the resource acquisition.

Xinxiang Li made contributions to the conceptualization, visualization, and writing—review & editing.

Zhiqian Hu made contributions to the funding acquisition, visualization, and writing—review & editing.

Xinxing Li made contributions to the investigation, resource acquisition, visualization, writing—original draft, and writing—review & editing.

All authors read and approved the final manuscript.

ACKNOWLEDGEMENTS

We would like to thank Prof. Weiping Chen (Zhejiang Cancer Hospital) for English language editing.

CONFLICT OF INTEREST STATEMENT

The authors declare that they have no competing interests.

FUNDING INFORMATION

The authors gratefully acknowledge the financial support from the National Key R&D Program of China (No. 2019YFA0110601), National Natural Science Foundation of China (No. 81571827), Natural Science Foundation Project of Shanghai Science and Technology Commission (SKW2030), Excellent Discipline Reserve Talent Plan of Tongji Hospital Affiliated to Tongji University (HBRC2014), Clinical research Project of Tongji Hospital Affiliated to Tongji University (ITJ-ZD-2104), Key talent introduction project of Tongji Hospital Affiliated to Tongji University (RCQD2102), Talent project of Tongji Hospital Affiliated to Tongji University (GJPY2111), and Shanghai Tongji Hospital special disease database construction project (TJ-DB-2105).

DATA AVAILABILITY STATEMENT

The data that support the findings of this study are available on request from the corresponding author on reasonable request.

ETHICS APPROVAL AND CONSENT TO PARTICIPATE

All the investigation protocols were approved by the Institutional Ethics Committees of Shanghai Changzheng Hospital and Shanghai Tongji Hospital (SBKT-2022-155). All subjects provided informed consent to participate in the study and approved the use of their biological samples for analysis. All experiments were performed following institutional guidelines, in compliance with relevant laws. Data sharing mechanisms will ensure that the rights and privacy of individuals participating in research will be guaranteed.

Haiyang Zhou¹

Jiahui Yin²

Anqi Wang¹

Xiaomao Yin³

Taojun Jin⁴


Kai Xu³

Lin Zhu³

Jiexuan Wang³

Wenqiang Wang³

Wei Zhang³

Xinxiang Li^{5,6}
 Zhiqian Hu^{1,3}
 Xinxiang Li³ 

¹*Division of Colorectal Surgery, Changzheng Hospital, Navy Medical University, Shanghai, P. R. China*

²*Institute of Higher Education, Tongji University, Shanghai, P. R. China*

³*Department of Gastrointestinal Surgery, Tongji Hospital, Tongji University School of Medicine, Shanghai, P. R. China*

⁴*Department of Gastroenterology, Shuguang Hospital, Shanghai University of Traditional Chinese Medicine, Shanghai, P. R. China*

⁵*Department of Colorectal Surgery, Fudan University Shanghai Cancer Center, Shanghai, P. R. China*

⁶*Department of Oncology, Shanghai Medical College, Fudan University, Shanghai, P. R. China*

Correspondence

Xinxiang Li, Department of Gastrointestinal Surgery, Tongji Hospital, Tongji University School of Medicine, Shanghai 200065, P. R. China.
 Email: ahtxxx2015@163.com

Zhiqian Hu, Division of Colorectal Surgery, Changzheng Hospital, Navy Medical University & Department of Gastrointestinal Surgery, Tongji Hospital, Tongji University School of Medicine, Shanghai 200065, P. R. China.
 Email: huzhiq163@163.com

Xinxiang Li, Department of Colorectal Surgery, Fudan University Shanghai Cancer Center & Department of Oncology, Shanghai Medical College, Fudan University, Shanghai 200032, P. R. China.
 Email: xinxiangli@fudan.edu.cn

Haiyang Zhou, Jiahui Yin, and Anqi Wang contributed equally.

ORCID

Xinxiang Li  <https://orcid.org/0009-0007-9586-327X>

REFERENCES

1. Kranenburg O, van der Speeten K, de Hingh I. Peritoneal Metastases from Colorectal Cancer: Defining and Addressing the Challenges. *Front Oncol.* 2021;11:650098.
2. Sugarbaker PH. Prevention and Treatment of Peritoneal Metastases: a Comprehensive Review. *Indian J Surg Oncol.* 2019;10(1):3–23.
3. Dahlmann M, Gambara G, Brzezicha B, Popp O, Pachmayr E, Wedeken L, et al. Peritoneal metastasis of colorectal cancer (pmCRC): identification of predictive molecular signatures by a novel preclinical platform of matching pmCRC PDX/PD3D models. *Mol Cancer.* 2021;20(1):129.
4. Khaliq AM, Erdogan C, Kurt Z, Turgut SS, Grunvald MW, Rand T, et al. Refining colorectal cancer classification and clinical stratification through a single-cell atlas. *Genome Biol.* 2022;23(1):113.
5. Izar B, Tirosh I, Stover EH, Wakiro I, Cuoco MS, Alter I, et al. A single-cell landscape of high-grade serous ovarian cancer. *Nat Med.* 2020;26(8):1271–1279.
6. Peterson VM, Castro CM, Chung J, Miller NC, Ullal AV, Castano MD, et al. Ascites analysis by a microfluidic chip allows tumor-cell profiling. *Proc Natl Acad Sci U S A.* 2013;110(51):e4978–e4986.
7. Carvalho RF, do Canto LM, Abildgaard C, Aagaard MM, Tronhjem MS, Waldstrøm M, et al. Single-cell and bulk RNA sequencing reveal ligands and receptors associated with worse overall survival in serous ovarian cancer. *Cell Commun Signal.* 2022;20(1):176.
8. Wang X, Yuwen TJ, Zhong Y, Li ZG, Wang XY. A new method for predicting the prognosis of colorectal cancer patients through a combination of multiple tumor-associated macrophage markers at the invasive front. *Heliyon.* 2023;9(2):e13211.
9. Ramirez DE, Mohamed A, Huang YH, Turk MJ. In the right place at the right time: tissue-resident memory T cells in immunity to cancer. *Curr Opin Immunol.* 2023;83:102338.
10. Li Z, Liu J, Chen H, Zhang Y, Shi H, Huang L, et al. Ferritin Light Chain (FTL) competes with long noncoding RNA Linc00467 for miR-133b binding site to regulate chemoresistance and metastasis of colorectal cancer. *Carcinogenesis.* 2020;41(4):467–477.

SUPPORTING INFORMATION

Additional supporting information can be found online in the Supporting Information section at the end of this article.